Display of Haptic Shape Using Ultrasound Pressure Distribution Forming Cross-Sectional Shape

Atsushi Matsubayashi[1], Hiroki Oikawa[1], Saya Mizutani[2], Yasutoshi Makino[2], and Hiroyuki Shinoda[2]

Abstract— In this paper, we propose a method for expressing the shape of a virtual object using ultrasound tactile presentation. In this method, the cross-sectional shape of a finger penetrating the virtual object is estimated from a point cloud acquired by a depth sensor. An ultrasound focus is moved around the cross-sectional shape at a high speed, which enables the generation of a pressure distribution on the finger corresponding to the position of the object surface. This method can be applied to any 3D polygon mesh model, and the local shape of the model can be recognized from the change in the pressure distribution when the finger is inserted into it. We conducted a numerical simulation and a user study to verify the effectiveness of this method for object shape recognition.

I. INTRODUCTION

The recent development of technology to display mid-air images can achieve a contactless interface. Although an aerial interface that changes the function according to the displayed image is clean and flexible, lack of haptic feedback reduces its operability. Mid-air tactile presentation technology has a possibility to solve this problem. If the shape of buttons and knobs are expressed by mid-air tactile display, the user can intuitively operate them in a manner similar to everyday life. Furthermore, virtual objects with haptic shapes enable manipulation of the interface only with tactile information. As shown in Fig. 1 (a), in situations where the user cannot keep an eye on the control panel such as cockpit of a car, an airborne tactile presentation allows the user to operate controls floating in the air by recognizing the shape of them.

As airborne tactile presentation techniques, air jet [1], vortex ring [2], laser [3][4], and ultrasound waves [5] have been proposed. Among these, ultrasound approach has higher spatial and temporal resolution. By controlling the phase of the ultrasound transducers, it is possible to generate a focal point at any position in the space. When the focal point is blocked by a human body, a tactile sensation is evoked based on the acoustic radiation pressure. However, as the generated force is weak (1.6 $\mathrm{gf/cm^2}$ with 324 transducers [6]), it is inevitable for the finger to penetrate the virtual object, and it is difficult to recognize the shape of the object by tracing its surface with the finger.

We had previously proposed a mid-air haptic 3D manipulation system [7], which can present a surface position of a

[1]A. Matsubayashi and H. Oikawa are from Graduate School of Information Science and Technology, The University of Tokyo, 7-3-1 Hongo, Bunkyo-ku, Tokyo 113-8654 Japan.
[2]S. Mizutani, Y. Makino, and H. Shinoda are fromGraduate School of Frontier Sciences, The University of Tokyo, 5-1-5 Kashiwanoha, Kashiwa-shi, Chiba 277-8561 Japan
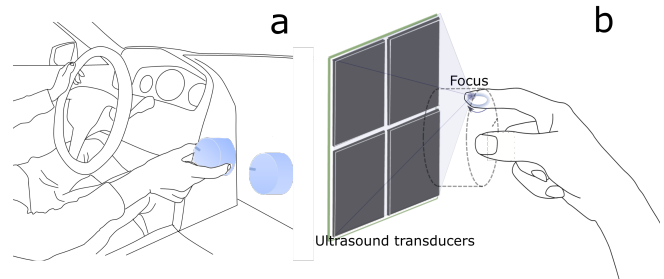

Fig. 1.   (a) An airborne tactile presentation allows the user to operate controls without watching it, (b) A pressure distribution forming the cross-sectional shape is generated on the finger surface by moving the focus of the ultrasound around it

3D object to the user by generating a pressure distribution on the surface of the finger that forms a cross-sectional shape of the object and the finger. However, the method used in this system works correctly only when touching a surface larger than the finger and cannot represent complex surfaces. In this paper, we extend this method to be applicable to all polygon mesh objects. In this method, from a point cloud of the finger surface acquired by the depth sensor, points located near the polygon surface are extracted, and a time-averaged pressure distribution forming the cross-sectional shape is generated by moving the ultrasound focus along these points at a high speed as shown in Fig. 1 (b). When the work space is surrounded by a large number of transducers, the diameter of ultrasound focal point is suppressed to about 5 mm, so that the generated distribution can be sufficiently detailed to perceive cross-sectional shape. The user can estimate the shape of the object by detecting the roundness and corners of the object surface, from the change in pressure distribution according to penetration of the finger, which is difficult to represent by the previous method [7]. To evaluate the effectiveness of our method quantitatively, we conducted a numerical simulation and a user study. Simulation results showed that the pressure distribution generated on a fingertip by the proposed algorithm differs depending on the shape of the object. The result of the user study indicated that the shape of some objects can be recognized by slightly penetrating a fingertip vertically into the surface.

II. RELATED WORKS

several methods for presenting haptic shapes of virtual objects using ultrasound waves have been proposed. In some methods, haptic shapes are generated by controlling sound pressures on control points set in space. Hoshi et

al. proposed Fourier transform based technique to generate sound pressure field on a two-dimensional plane. Gavrilov proposed a method for generating multiple focal points to shape two-dimensional geometry [8]. In this method, by introducing the control point where the sound pressure is zero, Carter et al. decreased an unwanted peak of sound pressure. Hasegawa et al. proposed a method to generate a three-dimensional distribution with transducers located in a three-dimensional disposition [9]. Inoue et al. used three-dimensionally arranged transducers and solved phase retrieval problem to generate a standing haptic image [10]. These methods generate a sound field that forms a static shape in the air, hence it is possible to touch the object freely without hand tracking. However, as the sound pressure is widely distributed, the force applied to the hand is weak. Besides, it is difficult to express the sharp pressure change while touching the object, due to low spatial resolution of the haptic image.

In contrast, few methods for controlling the sound pressure on the surface of the hand or finger tracked by a sensor have been proposed. Inoue et al. proposed a method to control the sound pressure distribution on a polygon mesh model of a finger [11]. Although this method enables to generate the desired sound pressure distribution on the finger surface by creating a mesh model from the tracking data, computational cost is too high to apply in real-time. Long et al. proposed a method for generating multi-focus at the intersection of the hand with the object [12]. They demonstrated the effectiveness of this method for shape recognition, however in the experiment they used a simplified hand model with multiple quadrilaterals, hence it is difficult to set the focal positions on the finger surface properly. We have proposed a system that achieved interaction with 3D image [7]. This system estimated the cross-sectional shape of the finger in contact with a virtual object using ellipse regression of a point cloud, and generated pressure distribution on the finger by revolving an ultrasound focus around the ellipse. Although we showed that this method was effective in recognizing the position and angle of the object surface, this method is applicable only when touching a face larger than the fingertip. In this study, we extend this method to be applicable to any object expressed by polygon mesh. This extended method allows recognizing the corners and edges of the object.

III. ALGORITHM

In our method, the cross-sectional shape of a finger and a virtual object is estimated from the point cloud representing the hand measured by depth sensors, and a pressure distribution on the finger surface is generated by moving an ultrasound focus around the cross section at high speed. This process is performed in the following order.

1) From the obtained point cloud, points within a certain distance from the surface of the object are extracted and regarded as the ones forming the cross-sectional shape.
2) N positions where the focal point is generated, are determined to be equally distributed around the cross

section.
3) The phases and amplitudes of the ultrasound transducers are controlled so that a single focus moves the N positions sequentially.

We describe each of these algorithms in detail below.

A. Estimating Cross-Sectional Shape

A point cloud representing the hand shape can be obtained by reprojecting a depth image captured by the depth sensor in three-dimensional space. From the point cloud, the points inside the object whose distance to the object surface is less than a certain threshold value δ are extracted as shown in Fig. 2 (a). Consider a case where the object is represented by a convex polygon mesh composed of M faces. Let $\mathbf{x}_i \in \mathbb{R}^3$ be the position of the point i, and $\mathbf{n}_m \in \mathbb{R}^3$ and $\mathbf{x}_m \in \mathbb{R}^3$ be the normal unit vector and the centroid of the face m, respectively. If

$$
\begin{aligned}
(\forall m \quad & (\mathbf{x}_m - \mathbf{x}_i) \cdot \mathbf{n}_m > 0) \\
\wedge \quad & (\exists m \quad \delta > (\mathbf{x}_m - \mathbf{x}_i) \cdot \mathbf{n}_m > 0),
\end{aligned} \tag{1}
$$

then the point i is extracted. As this process is independent for each point, it can be processed at high speed by parallel calculation using a multi-core CPU or GPU.

B. Determining Focal Positions

The extracted point cloud is considered for shaping the cross section. N focal positions are determined to be evenly distributed in this point cloud. First, principal component analysis is performed on the obtained point cloud, and each point is projected onto the plane orthogonal to the third principal component . Let $\mathbf{x}_i \in \mathbb{R}^3, i = \{1, \cdots, I\}$ and $\overline{\mathbf{x}} \in \mathbb{R}^3$ be the position of the point i in the cross section and the centroid, respectively. The eigen value decomposition of variance-covariance matrix of the points is described as

$$
\frac{1}{I}\overline{\mathbf{X}}^{\mathrm{T}}\overline{\mathbf{X}} = \mathbf{W}\mathbf{\Lambda}\mathbf{W}^{\mathrm{T}} = (\mathbf{w}_1, \mathbf{w}_2, \mathbf{w}_3)\begin{pmatrix} \lambda_1 & & \\ & \lambda_2 & \\ & & \lambda_3 \end{pmatrix}\begin{pmatrix} \mathbf{w}_1^{\mathrm{T}} \\ \mathbf{w}_2^{\mathrm{T}} \\ \mathbf{w}_3^{\mathrm{T}} \end{pmatrix}, \tag{2}
$$

where

$$
\overline{\mathbf{X}} = (\mathbf{x}_1 - \overline{\mathbf{x}}, \cdots, \mathbf{x}_I - \overline{\mathbf{x}})^{\mathrm{T}} \tag{3}
$$

$$
\lambda_1 \geq \lambda_2 \geq \lambda_3 \geq 0. \tag{4}
$$

Each point $\mathbf{x}_i$ is projected on the plane formed by the first and second principal components such that the variance in each component direction is equal. The projected point $\mathbf{x}_i^* \in \mathbb{R}^2$ is calculated as

$$
\mathbf{x}_i^* = \begin{pmatrix} \frac{1}{\sqrt{\lambda_1}}\mathbf{w}_1^{\mathrm{T}} \\ \frac{1}{\sqrt{\lambda_2}}\mathbf{w}_2^{\mathrm{T}} \end{pmatrix}(\mathbf{x}_i - \overline{\mathbf{x}}). \tag{5}
$$

Then, as shown in Fig. 2 (c), the points $\mathbf{x}_i$ are divided into N clusters based on the angle of the projected point $\mathbf{x}_i^*$. The centroid of each cluster is taken as the position
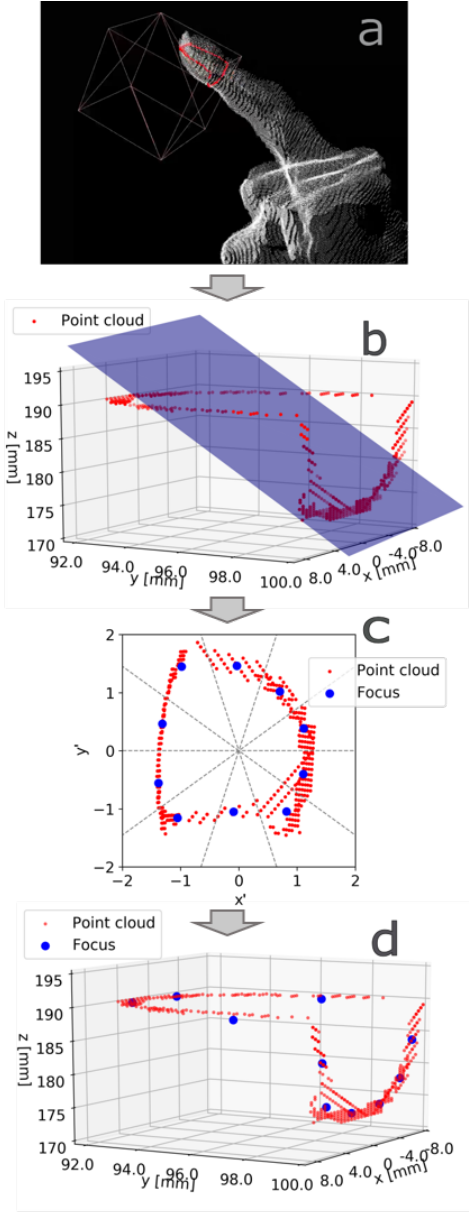
Fig. 2. (a) The points within a certain distance from the surface of the object are extracted (red). (b) Principal component analysis is performed to determine the plane to be projected. (c) The projected points are divided into clusters based on the angle. (d) The centroid of each cluster is taken as a focal position

where ultrasound focus will be generated. The position of ultrasound focus $\mathbf{c}_n \in \mathbb{R}^3, n = \{1, \cdots, N\}$ is calculated as

$$\mathbf{c}_n = \frac{1}{|C_n|} \sum_{i \in C_n} \mathbf{x}_i \tag{6}$$

$$C_n = \left\{ i \ \middle| \ \frac{2\pi(n-1)}{N} \le \arg\left(\mathbf{x}_i^*\right) < \frac{2\pi n}{N} \right\}, \tag{7}$$

where $\arg\left(\mathbf{x}_i^*\right) \in [0, 2\pi)$ represents the clockwise angle of $\mathbf{x}_i^*$ from $\left(1, 0\right)^{\mathrm{T}}$. Fig. 2 (d) shows focal positions calculated
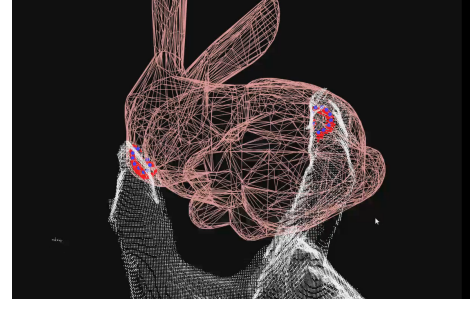

Fig. 3. Our algorithm can be applied to any objects touched with any number of fingers.

C. Generating Ultrasound Focus

The phases and amplitudes of the ultrasound transducers are controlled to generate a single focus that moves the N positions sequentially. Let $\mathbf{x}_k \in \mathbb{R}^3, k = \{1, \cdots, K\}$ be the position of each transducer. To generate a focus at the position $\mathbf{c}_n$, the complex amplitude of each transducer $q_k \in \mathbb{C}$ is set as

$$q_k = \|\mathbf{c}_n - \mathbf{x}_k\| e^{2\pi i \frac{f}{c} \|\mathbf{c}_n - \mathbf{x}_k\|},$$

where c is the speed of sound and f is the frequency of the ultrasound waves. There is arbitrariness in the N number of focal positions and the order of the positions to move. These affect the spatial smoothness of the pressure distribution generated on a finger and the frequency components of the vibrotactile sensation. They should be chosen according to the implementation environment, which is described in detail in the next section.

D. Extension to general objects

Although only convex objects have been considered so far, it is possible to apply the same algorithm by dividing a concave object into multiple convex objects. Furthermore, by clustering a point cloud inside the object and applying this algorithm separately for each cluster, it is possible to touch the object using multiple fingers. By creating multiple focal points and moving them independently, it is possible to present tactile sensations to multiple fingers.

In our setup, we implemented the VHACD algorithm [13] to decompose concave object to multiple convex hulls and distance-based clustering algorithm in Point Cloud Library[14] to enable multi-finger touch. Fig. 3 shows a situation where the divided Stanford Bunny is touched with two fingers.

IV. EXPERIMENT

To evaluate the effectiveness of our method in recognizing an object shape, we conducted a numerical simulation and a user study.

A. Experimental Setup

We constructed a system as shown in Fig. 4 to conduct the experiment. We installed Intel RealSense Depth Camera D415 [15] to measure the hands of the participants. The
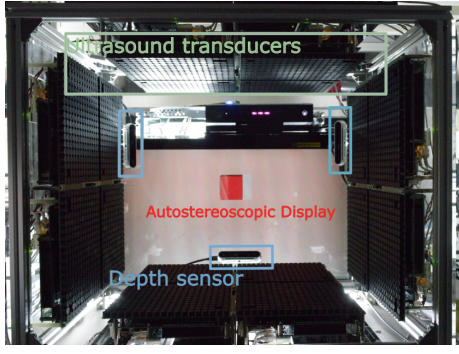
Fig. 4. Our setup of experiment. Three depth sensors capture a hand shape. A total of 3984 small transducers enclosed the workspace. An autostereoscopic display is placed behind the workspace.

Fig. 5. The coordinate system and the arrangement of the ultrasound transducers in our setup.

resolution of the depth image captured by each camera is 848 × 480, and the refresh rate is 90 Hz. we set three cameras to acquire the depth information of all sides of the hand. A total of 3984 ultrasound transducers were arranged to surround the work space. The architecture of the ultrasound transducer array unit used in the system is that proposed by Inoue et al [16]. the resonant frequency of the transducer is 40 kHz. The focus update interval of the transducers is set to 1.5 ms. To express the objects visually, an autostereoscopic display, which is created by Kakeya et al. [17], is placed behind the workspace. The algorithms were implemented with OpenCL on Radeon Pro WX7100 GPU.

The threshold value δ for extracting point cloud is set to 1.5 [mm]. The number of focal positions N is set to 10, and the focus revolves every third point out of the 10 points. It is possible to create a sufficiently smooth distribution on the finger surface with 10 focal positions. On revolving every three points, the focal point revolving on the finger surface is 200 times per second, hence the 200 Hz component of the vibrotactile stimulus is dominant, to which a tactile mechanoreceptor is the most sensitive [18].

B. Numerical Simulation

We numerically simulated the acoustic radiation pressure distribution generated at the fingertip when it touched the haptic object expressed using our method. The pressure distribution on the mesh model, which is 5 cm from the tip of the finger and composed of 4322 faces, was calculated using the Boundary Element Method (BEM). The numerical calculation method is the same as that used by Inoue et al. [11]. Fig. 5 shows the coordinate system and arrangement of the ultrasound transducers in our setup. Fig. 6 (1a)-(4a) shows the focal position determined by our algorithm. The vertices of the finger model were regarded as a point cloud obtained from a depth sensor. The finger penetrates about 3 mm into all the four types of objects (cube, semi-sphere, pyramid and prism). The sides of the cube are 4 cm each. The radius of the semi-sphere is 2 cm. The bottom face of the pyramid and the prism is a square with a side of 4 cm, and the top angle is 45. Each object is placed such that the y coordinate of the top is 0.
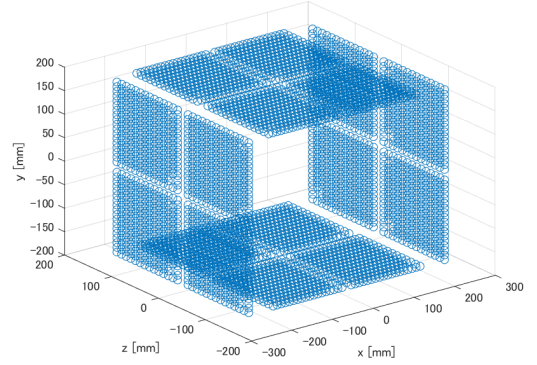
Fig. 6 (1b)-(4b) shows the time-averaged pressure distribution spread on the fingertip. It can be seen that the pressure distributions are generated along the cross-sectional shape of the finger and the object. The size and shape of the place with large pressure differ depending on the shape of the object. When touching the cube, the pressure distribution forms the cross-sectional shape that spreads over the fingertip , while touching the pyramid, the pressure distribution is generated almost by a single focus of about 5 mm in radius. These results suggest the possibility of identifying the object shape by just touching the top slightly.

C. User Study

In this experiment, participants performed tasks such as touching and identifying four types of objects (cube, semi-sphere, pyramid and prism) expressed using our method. The shape and position of the objects were similar to the ones used in the numerical simulation. In the experiment, we compared the proposed method to the method of generating only one focus at the centroid of the extracted point cloud representing the cross-sectional shape. In the single focus method, amplitude modulation at 200 Hz was applied to give a perceptible vibrotactile sensation. To prevent the influence of noise during tactile presentation, the participants performed tasks of hearing the white noise with headphones as shown in Fig. 7 (a).

1) Procedure: First, to know the shape of the object used in the experiment, the participants were asked to touch the object displayed on the 3D display. As shown in Fig. 7 (b), a small tile is displayed as a marker on the top of the object. The participants were asked to move the finger up and down from the marker. However, they could touch only the upper part of the object. While the point captured by the depth sensors existed below 1.5 cm from the top of the object, the tactile presentation was stopped. The time given for touching was 10 s, and the process was repeated for each of the four shapes. Next, the participants were given 3 min to touch the object only using tactile sense. The 3D display showed only the marker, as demonstrated in Fig. 7 (c). The way of touching the object is similar to the one discussed
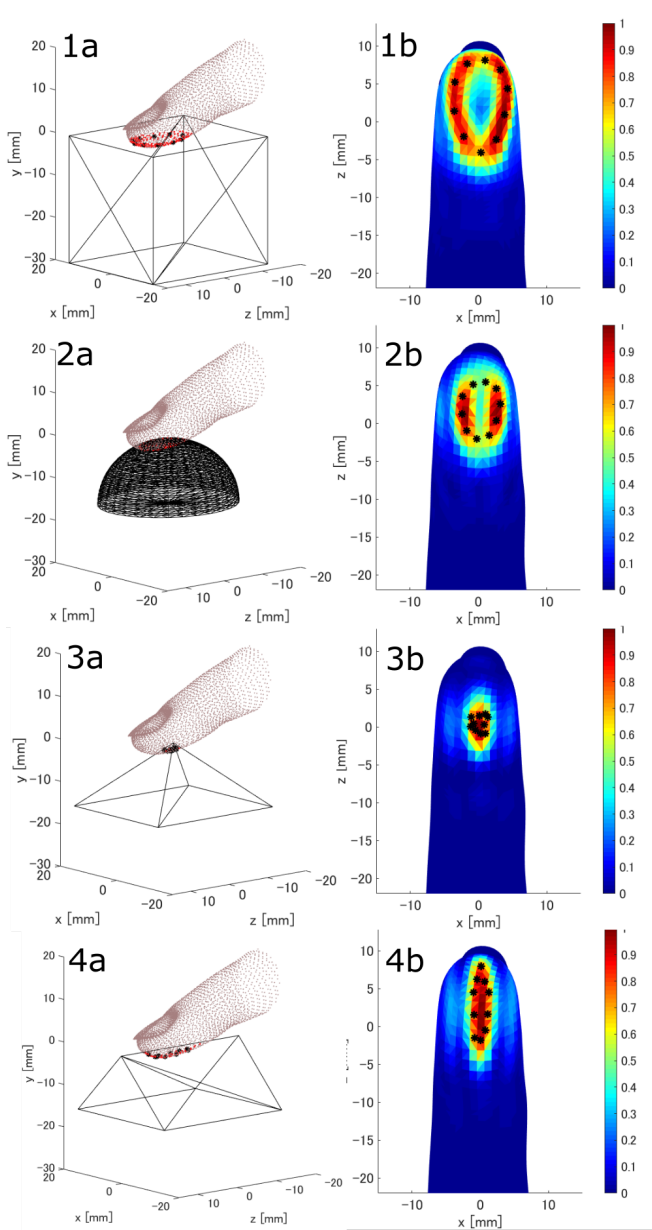
Fig. 6. (1a)-(4a) The algorithm extracts the points inside the object (red) and determines the 10 focal positions (asterisks). (1b)-(4b) The result of the numerical simulation. The value is the average of the distributions generated by 10 focal points at the positions marked by asterisks. The distribution is normalized by the maximum value.
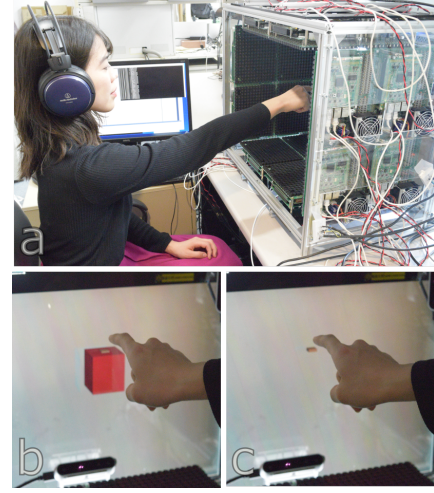

Fig. 7. The user study setup: (a) The participants heard white noise while performing tasks. (b) At the beginning of the experiment, the participants touched the object displayed on the 3D display. (c) While performing tasks, only the marker was displayed.
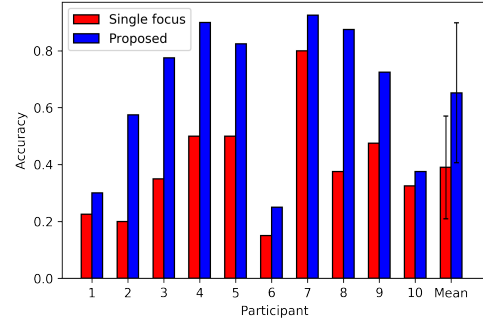

Fig. 8. Accuracy rates of the participants and the corresponding mean value. The error bar denotes standard deviation.

previously. During this time, the participants could change the shape of the object freely with a keyboard operation and perceive differences in tactile sensation perceived on their fingers. Then, the participants were asked to repeatedly perform the tasks to identify the shape using only tactile sensation. Similar to the previous situation, the participants were allowed to move their fingers only vertically from the marker. After 10 s of touching, the tactile presentation was stopped, and participants answered the shape from the four options. Participants performed a task once as a practice and then performed 10 tasks for each shape (total 40 tasks).

In either case, no answer was taught to the participants. In practice, the shape is set to semi-sphere. The order of the 40 tasks is randomized. The above process was done separately under two methods to avoid confusion between methods. Five of the ten participants performed the experiment with proposed method and the other five performed the experiment with single focus method.

2) Result: Ten participants (six males and four females), aged between 22 to 26, took part in the experiment. Fig. 8 shows the accuracy rate of the participants. The participant 1 to 5 performed the experiment using the single focus method first and the participant 6 to 10 performed the experiment using the proposed method first. The mean value of the accuracy rates among participants was 0.390 in the single focus method and 0.653 in the proposed method, and the Wilcoxon signed-rank test yielded a significant difference ($p < 0.01$) between the two methods. Table I,II showed the confusion matrix in each method.

3) Discussion: The results show that the proposed method has a higher accuracy rate than the single focus method for all the participants as well shapes. Considering the results of the numerical simulation, it is suggested that the shape of

TABLE I

CONFUSION MATRIX UNDER THE SINGLE FOCUS METHOD

actual \predicted	cube	semi-sphere	pyramid	prism
cube	0.50	0.30	0.09	0.11
semisphere	0.23	0.42	0.16	0.19
pyramid	0.13	0.37	0.26	0.24
prism	0.17	0.18	0.27	0.38

TABLE II

CONFUSION MATRIX UNDER THE PROPOSED METHOD

actual \predicted	cube	semi-sphere	pyramid	prism
cube	0.74	0.14	0.02	0.10
semisphere	0.05	0.59	0.11	0.25
pyramid	0.02	0.30	0.65	0.03
prism	0.14	0.10	0.13	0.63

the object can be estimated from the pressure distribution generated on the finger surface by the proposed method. In the single focus method, as the focus is on the centroid of the point cloud, the participants could estimate only the height of the cross section from the direction in which the pressure is felt. Therefore, it is considered that the accuracy rate of the cube is higher because the change in the height of the cross section with respect to the finger is larger in the movement of 1.5 cm. Similarly, the confusion matrix of the proposed method shows a high accuracy rate of the cube. Furthermore, in addition to height, information on the shape of the cross-section was also given to the participants in the proposed method, so the accuracy rate of the pyramid and the prism, which have characteristic cross-sectional shapes (small or narrow), are much higher than single focus method. The accuracy rate varies significantly among the participants, while the correlation between the methods is high (the correlation coefficient $r = 0.77$). It appears that the way of receiving information by tactile sensation was different for each participant. In this experiment, we did not give instructions on the appropriate speed of touching or on the distinctive features of the objects. We may be required to verify if the accuracy rate could sufficiently change with adequate instructions and training.

V. CONCLUSION

In this paper, we proposed a method to generate pressure distribution based on the cross-sectional shape of a finger. The results of the numerical simulation and the user study showed that our method is effective in shape recognition.

Since our method enables the touching of any object represented by polygon mesh, it can be easily combined with 3D display technology. Touchable stereoscopic images have the possibility of being constructed with various natural and intuitive interfaces. For example, when 3D modeling or designing is performed using such interfaces, it is possible to work without being concern about the occlusion problem as the recognition of the shape and position of the object is done with touching. Furthermore, if it is possible to express weight of an object or texture of a surface tactilely, the operability of the interface can be further improved. Our next step is to

present such information to the user with ultrasound tactile presentation.

REFERENCES

[1] Y. Suzuki and M. Kobayashi, "Air jet driven force feedback in virtual reality," *IEEE computer graphics and applications*, vol. 25, no. 1, pp. 44–47, 2005.

[2] G.-Z. Wang, Y.-P. Huang, T.-S. Chang, and T.-H. Chen, "Bare finger 3d air-touch system using an embedded optical sensor array for mobile displays," *Journal of Display Technology*, vol. 10, no. 1, pp. 13–18, 2014.

[3] H.-S. Kim, J.-S. Kim, G.-I. Jung, J.-H. Jun, J.-R. Park, S.-P. Kim, S. Choi, S.-J. Park, M.-H. Choi, and S.-C. Chung, "Evaluation of the possibility and response characteristics of laser-induced tactile sensation," *Neuroscience letters*, vol. 602, pp. 68–72, 2015.

[4] Y. Ochiai, K. Kumagai, T. Hoshi, J. Rekimoto, S. Hasegawa, and Y. Hayasaki, "Fairy lights in femtoseconds: aerial and volumetric graphics rendered by focused femtosecond laser combined with computational holographic fields," *ACM Transactions on Graphics (TOG)*, vol. 35, no. 2, p. 17, 2016.

[5] T. Iwamoto, M. Tatezono, and H. Shinoda, "Non-contact method for producing tactile sensation using airborne ultrasound," in *Proceedings of the International Conference on Human Haptic Sensing and Touch Enabled Computer Applications*. Springer, 2008, pp. 504–513.

[6] T. Hoshi, M. Takahashi, T. Iwamoto, and H. Shinoda, "Noncontact tactile display based on radiation pressure of airborne ultrasound," *IEEE Transactions on Haptics*, vol. 3, no. 3, pp. 155–165, 2010.

[7] A. Matsubayashi, Y. Makino, and H. Shinoda, "Direct finger manipulation of 3d object image with ultrasound haptic feedback," in *Proceedings of the Conference on Human Factors in Computing Systems*. ACM, 2019 (accepted).

[8] L. R. Gavrilov, "The possibility of generating focal regions of complex configurations in application to the problems of stimulation of human receptor structures by focused ultrasound," *Acoustical Physics*, vol. 54, no. 2, pp. 269–278, 2008.

[9] K. Hasegawa and H. Shinoda, "A method for distribution control of aerial ultrasound radiation pressure for remote vibrotactile display," in *SICE Annual Conference , 2013 Proceedings of*. IEEE, 2013, pp. 223–228.

[10] S. Inoue, Y. Makino, and H. Shinoda, "Active touch perception produced by airborne ultrasonic haptic hologram," in *Proceedings of the World Haptics Conference*. IEEE, 2015, pp. 362–367.

[11] S. Inoue, Y. Makino, and h. Shinoda, "Mid-air ultrasonic pressure control on skin by adaptive focusing," in *International Conference on Human Haptic Sensing and Touch Enabled Computer Applications*. Springer, 2016, pp. 68–77.

[12] B. Long, S. A. Seah, T. Carter, and S. Subramanian, "Rendering volumetric haptic shapes in mid-air using ultrasound," *ACM Trans. Graph.*, vol. 33, no. 6, pp. 181:1–181:10, 2014-11.

[13] K. Mamou, "Volumetric hierarchical approximate convex decomposition," *Game Engine Gems 3*, 2016.

[14] R. B. Rusu and S. Cousins, "3d is here: Point cloud library (pcl)," in *Proceedings of the IEEE International Conference on Robotics and automation*. IEEE, 2011, pp. 1–4.

[15] (2018) Intel corporation. [Online]. Available: https://www.intel.com/

[16] S. Inoue, Y. Makino, and H. Shinoda, "Scalable architecture for airborne ultrasound tactile display," in *Proceedings of the International AsiaHaptics conference*. Springer, 2016, pp. 99–103.

[17] H. Kakeya, K. Okada, and H. Takahashi, "[papers] time-division quadruplexing parallax barrier with subpixel-based slit control," *ITE Transactions on Media Technology and Applications*, vol. 6, no. 3, pp. 237–246, 2018.

[18] P. Lamore, H. Muijser, and C. Keemink, "Envelope detection of amplitude-modulated high-frequency sinusoidal signals by skin mechanoreceptors," *The Journal of the Acoustical Society of America*, vol. 79, no. 4, pp. 1082–1085, 1986.